Inorg. Chem. **2003**, *42*, 6284–6293

Adduct Formation between Alkali Metal Ions and Anionic $LV^{V}O_2^-$ (L^{2-} = Tridentate ONS Ligands) Species: Syntheses, Structural Investigation, and Photochemical Studies†

Satyabrata Samanta,‡,§ Suman Mukhopadhyay,‡ Debdas Mandal,‡ Ray J. Butcher,|| and Muktimoy Chaudhury*,‡

Department of Inorganic Chemistry, Indian Association for the Cultivation of Science, Kolkata 700 032, India, and Department of Chemistry, Howard University, Washington, D.C. 20059

Received February 28, 2003

Syntheses of alkali metal adducts $[LVO_2M(H_2O)_n]$ (**1**–**7**) (M = Na^+, K^+, Rb^+, and Cs^+; L = L^1–L^3) of anionic *cis*-dioxovanadium(V) species (LVO_2^-) of tridentate dithiocarbazate-based Schiff base ligands H_2L (*S*-methyl-3-((5-(*R*-2-hydroxyphenyl))methyl)dithiocarbazate, R = H, L = L^1; R = NO_2, L = L^2; R = Br, L = L^3) have been reported. The LVO_2^- moieties here behave like an analogue of carboxylate group and have displayed interesting variations in their binding pattern with the change in size of the alkali metal ions as revealed in the solid state from the X-ray crystallographic analysis of **1**, **3**, **6**, and **7**. The compounds have extended chain structures, forming ion channels, and are stabilized by strong Coulombic and hydrogen-bonded interactions. The number of coordinated water molecules in $[LVO_2M(H_2O)_n]$ decreases as the charge density on the alkali metal ion decreases (n = 3.5 for Na^+ and 1 for K^+ and Rb^+, while, for Cs^+, no coordinated water molecule is present). In solution, compounds **1**–**7** are stable in water and methanol, while in aprotic solvents of higher donor strengths, viz. CH_3CN, DMF and DMSO, they undergo photoinduced reduction when exposed to visible light, yielding green solutions from their initial yellow color. The putative product is a mixed-oxidation (μ-oxo)divanadium(IV/V) species as revealed from EPR, electronic spectroscopy, dynamic ^1H NMR, and redox studies.

Introduction

The coordination chemistry of oxovanadium(IV) and -(V) species with *S*-methyl 3-((2-hydroxophenyl)methyl)dithiocarbazate and related molecules (H_2L^1–H_2L^3) as ONS donor ligands has been the topic our research in recent years.[1−5] These tridentate biprotic ligands can form a $LV^{IV}O$ (L = L^1–L^3) primary core with one or more available coordination site(s) for the acceptance of an ancillary ligand. We have recently established that aerial oxidation of these coordinatively unsaturated $LV^{IV}O$ precursors to anionic *cis*-dioxo $LV^{V}O_2^-$ products requires the mandatory presence of an organic base (:B) as a source of counterion (BH^+).[5,6] These protonated cations remain attached to the terminal oxo group(s)[5−7] of the LVO_2^- species, thereby enhancing its stability through charge neutralization. From a close similarity of electronic and molecular structures and coordination behavior, Floriani et al. have proposed the $LV^{V}O_2^-$ unit to be an "inorganic analogue" of carboxylate group.[8] The later is known to coordinate metal ions in a variety of modes (**I**–**III**) as shown in Chart 1. Many polynuclear and clustered coordination compounds have been reported recently[9] exploiting these coordination possibilities of the carboxylate group.

* To whom correspondence should be addressed. E-mail: icmc@mahendra.iacs.res.in.

† Dedicated to Professor K. Nag on the occasion of his 60th birthday.

‡ Indian Association for the Cultivation of Science.

§ Present address: Departments of Chemistry and Chemical & Environmental Engineering, University of California, Riverside, CA 92521.

|| Howard University.

(1) Dutta, S. K.; Samanta, S.; Ghosh, D.; Butcher, R. J.; Chaudhury, M. *Inorg. Chem.* **2002**, *41*, 5555.
(2) Dutta, S. K.; Samanta, S.; Mukhopadhyay, S.; Burckel, P.; Pinkerton, A. A.; Chaudhury, M. *Inorg. Chem.* **2002**, *41*, 2946.
(3) Dutta, S. K.; Samanta, S.; Kumar, S. B.; Han, O. H.; Burckel, P.; Pinkerton, A. A.; Chaudhury, M. *Inorg. Chem.* **1999**, *38*, 1982.
(4) Dutta, S. K.; Kumar, S. B.; Bhattacharyya, S.; Tiekink, E. R. T.; Chaudhury, M. *Inorg. Chem.* **1997**, *36*, 4954.
(5) Samanta, S.; Ghosh, D.; Mukhopadhyay, S.; Endo, A.; Weakley, T. J. R.; Chaudhury, M. *Inorg. Chem.* **2003**, *42*, 1508.
(6) Samanta, S.; Butcher, R. J., Chaudhury, M. Unpublished results.
(7) Dewey, T. M.; Du Bois, J.; Raymond, K. N. *Inorg. Chem.* **1993**, *32*, 1729.
(8) Giacomelli, A.; Floriani, C.; De Souza Duarte, A. O.; Chiesi-Villa, A.; Guastini, C. *Inorg. Chem.* **1982**, *21*, 3310.

10.1021/ic030080i CCC: $25.00
Published on Web 09/11/2003

Chart 1

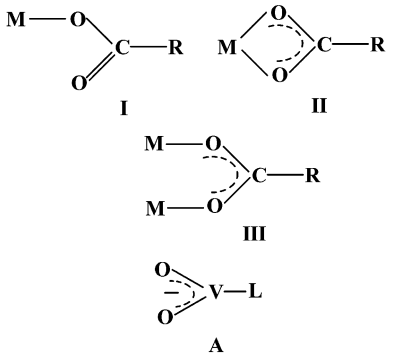

We, of late, have examined the coordination behavior of the $LV^VO_2^-$ (unit **A**) with sodium ion,[2] as a replacement for the protonated organic base ($:BH^+$). The product obtained is a single-stranded helicate $[L^1VO_2Na(H_2O)_2]_\infty$, where the $L^1VO_2^-$ units are attached to the sodium ions in a bis-monodentate fashion (mode **III**). Herein we report the coordination behavior of LVO_2^- ($L = L^1-L^3$) moieties toward some hard metal ions, belonging to group IA. Like the carboxylate group, the analogous LVO_2^- ligands have shown interesting diversity in molecular structure with the increase in size of the alkali metal ions (from Na^+ to Cs^+). Photochemical reactivity of these compounds has been examined in detail.

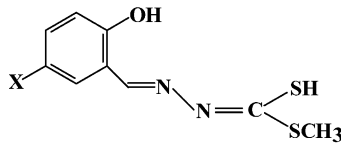

H_2L

X	H_2L
H	H_2L^1
NO_2	H_2L^2
Br	H_2L^3

Experimental Section

Materials. The ligands H_2L ($L = L^1-L^3$) were prepared as described elsewhere.[10] Rubidium carbonate and cesium carbonate were obtained from Aldrich. All other chemicals were commercially available and used as received.

Preparation of the Complexes. $[(L^3VO_2Na)_2(H_2O)_7]_\infty$ (1). To a stirred acetonitrile solution (10 mL) of $[VO(acac)_2]$ (0.26 g, 1 mmol) was added dropwise a solution of the ligand H_2L^3 (0.3 g, 1 mmol), also dissolved in acetonitrile (20 mL). The solution was heated at reflux for 10 min to give a clear brown solution. To this was then added an aqueous solution (5 mL) of sodium carbonate (0.13 g, 1.2 mmol), and the resulting solution was further refluxed for 1 h. The green solution obtained at this stage was filtered, and the filtrate was allowed to stand in the air for several days to become gradually yellow in color. The yellow solution after filtration was reduced to ca. 15 mL volume by rotary evaporation and refrigerated overnight at 4 °C to give a yellow microcrystalline product. It was collected by filtration, washed with Et_2O (4 × 10 mL), air-dried, and finally recrystallized from methanol. Drying under vacuum was avoided due to impending loss of water of crystallization. Yield: 0.25 g (56%). Anal. Calcd for $C_{18}H_{28}Br_2N_4Na_2O_{13}S_4V_2$: C, 22.88; H, 2.97; N, 5.93. Found: C, 23.2; H, 2.9; N, 6.0%. IR (KBr disk, cm^{-1}): ν(OH), 3400 b; ν(C⋯N), 1596 s; ν(C⋯O/phenolate), 1535 s; ν(V═O_t), 948, 900 s.

$[(L^2VO_2Na)_2(H_2O)_7]_\infty$ (2). An analogous method of preparation as described above for **1** was employed using the nitro derivative ligand (H_2L^2) that rendered isolation of **2** in 53% yield as a brown crystalline solid. Anal. Calcd for $C_{18}H_{28}N_6Na_2O_{17}S_4V_2$: C, 24.66; H, 3.20; N, 9.59. Found: C, 24.2; H, 3.1; N, 9.9. IR (KBr disk, cm^{-1}): ν(OH), 3432 s; ν(C⋯N), 1608 s; ν(C⋯O/phenolate), 1553 s; ν(V═O_t), 943, 891 s; ν(C−NO_2), 844 s.

$[L^1VO_2K(H_2O)]_\infty$ (3). To a solution of $[VO(acac)_2]$ (0.26 g, 1 mmol) in acetonitrile (10 mL) was added under stirring a solution of H_2L^1 (0.23 g, 1 mmol), also dissolved in the same solvent (20 mL). The solution was refluxed for 10 min, combined with an aqueous solution (5 mL) of potassium carbonate (0.17 g), and refluxed further for 1 h to give a green solution. It was filtered and the filtrate allowed to stand in the air for several days becoming gradually yellow in color. The yellow solution was rotary evaporated to near dryness, extracted with 2-propanol (15 mL), and filtered. The filtrate was cooled to 4 °C for an overnight period to give a yellow crystalline product. It was collected by filtration, washed with Et_2O (4 × 10 mL), and dried in the air. The product was recrystallized from 2-propanol. Yield: 0.19 g, (53%). Anal. Calcd for $C_9H_{10}KN_2O_4S_2V$: C, 29.67; H, 2.75; N, 7.69. Found: C, 28.9; H, 2.7; N, 7.4. IR (KBr disk, cm^{-1}): ν(OH), 3470 b; ν(C⋯N), 1604s; ν(C⋯O/phenolate), 1545 s; ν(V═O_t), 936, 888 s.

$[L^3VO_2K(H_2O)]_\infty$ (4). This compound was obtained in 64% yield by following a procedure identical with that mentioned above for **1** using K_2CO_3 as the alkali metal ion source instead of Na_2CO_3. Anal. Calcd for $C_9H_9BrKN_2O_4S_2V$: C, 24.38; H, 2.03; N, 6.32. Found: C, 24.6; H, 2.1; N, 6.3. IR (KBr disk, cm^{-1}): ν(OH), 3383 b; ν(C⋯N), 1599 s; ν(C⋯O/phenolate), 1536 s; ν(V═O_t), 947, 904 s.

$[L^1VO_2Rb(H_2O)]_\infty$ (5). This compound was prepared following an analogous procedure as mentioned above for **3** using rubidium carbonate as the source of alkali metal ion. Yield: 66%. Anal. Calcd for $C_9H_{10}N_2O_4RbS_2V$: C, 26.31; H, 2.44; N, 6.82. Found: C, 26.2; H, 2.3; N, 6.9. IR (KBr disk, cm^{-1}): ν(OH), 3400 b; ν(C⋯N), 1596 s; ν(C⋯O/phenolate), 1540 s; ν(V═O_t), 940, 900 s.

$[L^2VO_2Rb(H_2O)]_\infty$ (6). This compound was prepared using the same procedure as for **1** except that H_2L^2 and Rb_2CO_3 were used as the ligand and alkali metal ion source, respectively. Yield: 54%. Anal. Calcd for $C_9H_9N_3O_6RbS_2V$: C, 23.71; H, 1.98; N, 9.22. Found: C, 24.0; H, 1.9; N, 9.4. IR (KBr disk, cm^{-1}): ν(OH), 3300 b; ν(C⋯N), 1609 s; ν(C⋯O/phenolate); 1552 s; ν(V═O_t), 936, 884 s; ν(C−NO_2), 831 s.

$[L^1VO_2Cs]_\infty$ (7). This compound was prepared by following a procedure essentially identical with that described for **3** but with cesium carbonate being the source of alkali metal ion. Yield: 46%. Anal. Calcd for $C_9H_8CsN_2O_3S_2V$: C, 24.55; H, 1.82; N, 6.36. Found: C, 24.6; H, 1.8; N, 6.2. IR (KBr disk, cm^{-1}): ν(C⋯N), 1602 s; ν(C⋯O/phenolate), 1544s; ν(V═O_t), 944, 893 s.

(9) See for example: (a) Chang, A.; Francesconi, L. C.; Malley, M. F.; Kumar, K.; Gougoutas, J. Z.; Tweedle, M. F.; Lee, D. W.; Wilson, L. J. *Inorg. Chem.* **1993**, *32*, 3501. (b) Yukawa, Y.; Igarishi, S.; Yamano, A.; Sato, S. *Chem. Commun.* **1997**, 711. (c) Harben, S. M.; Smith, P. D.; Beddoes, R. L.; Collison, D.; Garner, C. D. *Angew. Chem., Int. Ed. Engl.* **1997**, *36*, 1897. (d) Powell, A. K.; Heath, S. L.; Gatteschi, D.; Pardi, L.; Sessoli, R.; Spina, G.; Del Giallo, F.; Pieralli, F. *J. Am. Chem. Soc.* **1995**, *117*, 2491. (e) Smith, P. D.; Berry, R. E.; Harben, S. M.; Beddoes, R. L.; Helliwell, M.; Collison, D.; Garner, C. D. *J. Chem. Soc., Dalton Trans.* **1997**, 4509.

(10) Dutta, S. K.; Tiekink, E. R. T.; Chaudhury, M. *Polyhedron* **1997**, *16*, 1863.

Table 1. Relevant Crystal Data for $[(L^3VO_2Na)_2(H_2O)_7]_\infty$ (**1**), $[L^1VO_2K(H_2O)]_\infty$ (**3**), $[L^2VO_2Rb(H_2O)]_\infty$ (**6**), and $[L^1VO_2Cs]_\infty$ (**7**)

	1	**3**	**6**	**7**
chem formula	$Na_2C_{18}H_{28}N_4Br_2S_4O_{13}V_2$	$KC_9H_{10}N_2S_2O_4V$	$RbC_9H_9N_3S_2O_6V$	$CsC_9H_8N_2S_2O_3V$
fw	944.36	364.35	455.72	440.14
cryst system	triclinic	orthorhombic	triclinic	monoclinic
space group	$P\bar{1}$	*Pbca*	$P\bar{1}$	$P2_1/c$
a, Å	7.739(2)	6.5705(9)	7.4650(9)	8.068(3)
b, Å	13.810(2)	13.506(2)	8.3921(10)	26.966(10)
c, Å	16.930(2)	31.332(4)	12.5586(15)	6.540(2)
α, deg	81.99(8)	90	91.74(2)	90
β, deg	89.80(13)	90	92.002(2)	110.57(3)
γ, deg	76.85(2)	90	107.074(2)	90
V, Å^3	1744.1(5)	2780.5(7)	750.95(16)	1332.7(9)
Z	2	8	2	4
density, ρ_{cal}, g·cm^{-3})	1.798	1.741	2.015	2.194
T, °C	20	20	20	20
λ, Å	0.710 73	0.710 73	0.710 73	0.710 73
F(000)	940	1472	448	480
abs coeff, mm^{-1}	3.152	1.321	4.189	3.749
θ range for data collection (deg)	2.43−54.04	3.02−27.49	1.62−28.35	2.70−25.00
reflcns collcd	8346	2861	5677	2509
indpdt reflcns (R_{int})	7855 (0.0273)	2861 (0.0000)	3553 (0.0185)	2308 (0.0670)
R1, wR2 (all data)	0.0436, 0.0850	0.0288, 0.0777	0.0310, 0.0817	0.0624, 0.1373

Physical Measurements. EPR spectra in solution at room temperature and in the frozen state (77 K) were recorded in X-band on a Bruker model ESP 300E spectrometer equipped with standard Bruker attachments. The ^{1}H NMR spectra were recorded on a Bruker model Avance DPX 300 spectrometer. Electronic spectra in the near-IR region were obtained on a Hitachi U-3400 UV−vis−NIR spectrophotometer. Solution electrical conductivity and IR and UV−vis spectra were obtained as described elsewhere.[11] Cyclic voltammetric measurements were performed on a PAR electrochemical analyzer (model 250/5/0) in dry acetonitrile under purified dinitrogen with tetraethylammonium perchlorate (TEAP) as the supporting electrolyte. A three-electrode configuration was employed with platinum working and counter electrodes. A saturated calomel electrode (SCE) was used for reference, and ferrocene, as an internal standard.[12]

Elemental analyses (for C, H, and N) were performed in this laboratory (at IACS) using a Perkin-Elmer 2400 analyzer.

Crystallography. Diffraction-quality crystals of **1**, **3**, **6**, and **7** were grown by slow evaporation from solutions in MeOH/H_2O (4:1 v/v) for **1**, 2-propanol for **3,** and neat methanol for **6** and **7**, respectively. Intensity data for the yellow fibrous crystals of **1** (0.11 × 0.70 × 0.12 mm), **3** (0.11 × 0.92 × 0.40 mm), and **7** (0.18 × 0.99 × 0.24 mm) were collected at room temperature on a Siemens P4 four-circle diffractometer using the $\theta-2\theta$ technique, while for **6** (0.15 × 0.47 × 0.55 mm) intensity data were collected on a Bruker 1K SMART CCD diffractometer, both diffractometers using graphite-monochromated Mo Kα X-radiation (λ = 0.710 73 Å) (details are given in Table 1). No crystal decay was observed during the data collection. The structures were solved by direct methods using *SHELXTLPC* package[13] of software for compounds **1**, **3**, and **7**, while for **6** *SMART* and *SHELXTL* programs[14] were used, as detailed elsewhere.[15,16] Final refinements were done by a full-matrix least-squares procedure based on all data minimizing R2 = $[\sum[w(F_o^2 - F_c^2)^2]/\sum[(F_o^2)^2]]^{1/2}$, R1 = $\sum||F_o| - |F_c||/\sum|F_o|$, and $S = [\sum[w(F_o^2 - F_c^2)^2]/(n - p)]^{1/2}$. All non-hydrogen atoms were refined as anisotropic, and the hydrogen atomic positions were fixed relative to the bonded carbons with isotropic thermal parameters fixed.

Photochemical Study. Clear yellow solutions of the complexes (**1**−**7**) in dry acetonitrile were taken in a quartz cell and purged with argon for 20 min. A tungsten filament lamp (60 W) was used as a visible light source to irradiate these solutions which gradually turned green with the passage of time during photolysis. The green solutions obtained after different intervals of exposure time were used for subsequent studies needed for their characterization.

Results and Discussion

Synthesis. The complexes **1**−**7** were prepared by the reaction of $[VO(acac)_2]$ with the tridentate ONS ligands ($H_2L^1-H_2L^3$) in CH_3CN/water medium in the presence of alkali metal carbonate. Obligatory steps in this preparative procedure are the presence of water in the reaction medium and its subsequent exposure to atmospheric oxygen as confirmed by several control experiments.[2] Details are summarized in Scheme 1. The reaction initially proceeds through a green vanadium(IV) intermediate which subsequently undergoes atmospheric oxidation to yellow *cis*-dioxovanadium(V) species. The reaction is very much dependent on carbonate anion as no other common alkali metal salts are found to be efficient enough to carry out such oxidation. The products obtained (**1**−**7**) have infinite chain structures in the solid state with interesting diversity in their compositions as confirmed by X-ray crystallography (see later), involving anionic LVO_2^- units coordinated like an analogue of carboxylate group to aquated alkali metal ions, except lithium. The cationic and anionic parts in these compounds are held together by the process of self-assembly[17] through the simultaneous use of Coulombic interactions and efficient hydrogen bonding. Similar bonding

(11) (a) Dutta, S. K.; McConville, D. B.; Youngs, W. J.; Chaudhury, M. *Inorg. Chem.* **1997**, *36*, 2517. (b) Bhattacharyya, S.; Weakley, T. J. R.; Chaudhury, M. *Inorg. Chem.* **1999**, *38*, 633.
(12) Gagné, R. R.; Koval, C. A.; Lisensky, G. C. *Inorg. Chem.* **1980**, *19*, 2854.
(13) Sheldrick, G. M. *SHELXLTLPC and SHELXTL*; *Program for Crystal Structure Determination*; Cambridge University: Cambridge, England, 1996.
(14) *SMART (Version 5.624) and SHELXTL (Version 5.10)*; Bruker AXS Inc.: Madison, WI, 2001.
(15) Eddington, N. D.; Cox, D. S.; Roberts, R. R.; Butcher, R. J.; Edafiogho, I. O.; Stables, J. P.; Cooke, N.; Goodwin, A. M.; Smith, C. A.; Scott, K. R. *Eur. J. Med. Chem.* **2002**, *37*, 635.
(16) Gilardi, R.; Butcher, R. J.; Bashir-Hashemi, A. *Acta Crystallogr.* **2002**, *E58*, 860.

Scheme 1

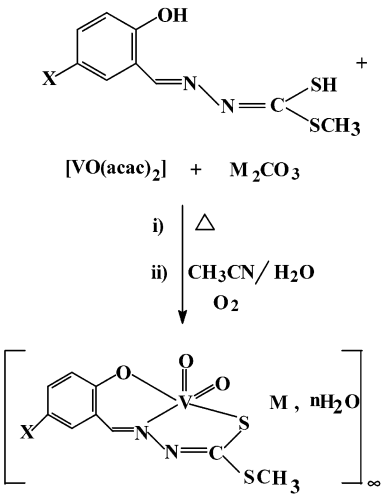

Complex	M	X	n
1	Na	Br	3.5
2	Na	NO_2	3.5
3	K	H	1
4	K	Br	1
5	Rb	H	1
6	Rb	NO_2	1
7	Cs	H	0

patterns have been systematically used in crystal engineering for the design and synthesis of organic supramolecular compounds.[18]

IR spectra of the complexes have all the characteristic bands of the coordinated tridentate (ONS) ligands.[4] In addition, the complexes display a strong two-band pattern, appearing in the 950−880 cm^{-1} region due to V═O_t terminal stretches, typical of the *cis*-VO_2 core.[19] A broad medium-intensity band in the high-frequency region 3400−3300 cm^{-1} indicates the presence of coordinated water molecules in **1**−**6**.

Description of Crystal Structures. The molecular structure of **1** reveals a hydrogen-bonded infinite assembly of stoichiometry $[(L^3VO_2Na_2(H_2O)_7)_2(L^3VO_2)_2]_\infty$ (Figure 1). The molecule contains a cationic (Figure 2) and an anionic part (Figure 3), both involving L^3VO_2 units which are structurally nonequivalent. Relevant metrical parameters are summarized in Table 2. Vanadium centers in both the parts have distorted square pyramidal geometry with donor atoms (S, N, and O) from the tridentate ligand and one of the terminal oxo atoms O(1B) [O(1A) for the anionic part] of the *cis*-VO_2 core forming the basal plane. The apical position is occupied by the remaining oxo ligand O(2B) [O(2A)] which forms angles in the range 100.24(14)−107.85(13)° [100.21(14)−109.3-(2)°] with the basal plane. The terminal V═O_t distances 1.612(3) and 1.662(3) Å [1.620(3) and 1.652(3) Å] and

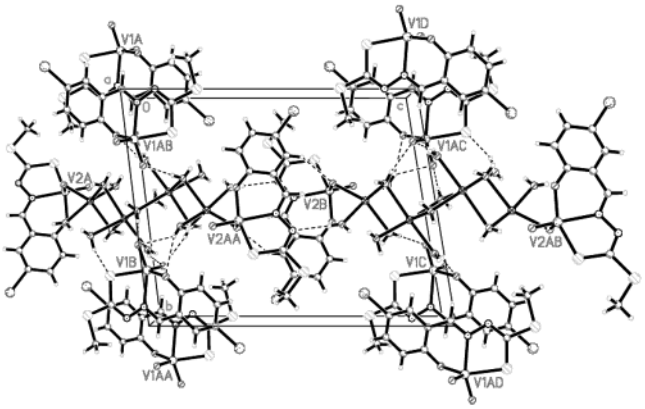

Figure 1. Molecular structure of $[(L^3VO_2Na)_2(H_2O)_7]_\infty$ (**1**) viewed along the *c* axis.

O(1)−V−O(2) angle 107.7(2)° [107.8(2)°] are in the expected range for a *cis*-VO_2 core.[19]

The cationic part of the complex is centrosymmetric (Figure 2) involving two L^3VO_2 units connected by a zigzag chain comprising four aquated sodium ion centers. The terminal sodium ion Na(1) has a trigonal bipyramidal geometry with the equatorial positions occupied by O(1W) and O(2W) from the two bridging aqua ligands in addition to a terminal oxo ligand O(2B) [Na(1)−O(2B), 2.447(3) Å] of a L^3VO_2 core. The axial positions are occupied by two more aqua ligands O(11W) and O(12W) of nonbridging type. The distances of Na(1) from O(1W), O(2W) and O(12W) are almost identical [in the range 2.352(4)−2.387(5) Å], while the remaining aqua ligand O(11W) is closer [Na(1)−O(11W), 2.284(5) Å] to the metal center. The sum of the three basal angles at sodium is 360°, and the Na(1) atom is displaced by 0.0323 Å from this least-squares basal plane toward the apical O(11W) atom.

Na(1) is connected to the central octahedral sodium ion Na(2) by the bridging oxygen atoms O(1W) and O(2W), the distances being Na(1)···Na(2) 3.566(3) Å, Na(2)−O(1W) 2.461(5) Å, and Na(2)−O(2W) 2.516(4) Å. The remaining coordination sites of Na(2) are occupied by two bridging O(23W), O(23W)$^{\#1}$ and two nonbridging O(21W), O(22W) aqua ligands with distances (Na−O(W)) in the range 2.383-(4)−2.454(4) Å. The former two oxo ligands are used to bind Na(2) with an identical atom Na(2)$^{\#1}$ of the other half of this centrosymmetric ion (Figure 2), the Na(2)···Na(2)$^{\#1}$ separation being 3.534(4) Å. Each cationic part, for charge counter balance, requires two anionic parts which remain interlocked by strong hydrogen bonding (Figure 1).

Crystallographic analysis of $[L^1VO_2K(H_2O)]_\infty$ (**3**) reveals an extended hydrogen-bonded structure as well. A perspective view of the monomeric unit is shown in Figure 4, and the relevant bonding parameters are in Table 3. The molecule when viewed along the *a* axis exhibits an infinite array of alternating $L^1VO_2^-$ and aquated K^+ ions, held together by strong hydrogen-bonding and Coulombic interactions (Figure 5). Individual vanadium(V) centers exist in a distorted square pyramidal geometry, as in **1**, with the basal positions being occupied by the donor atoms from the tridentate ligand together with a terminal oxo group O(2). The apical position

(17) (a) Lindsey, J. S. *New J. Chem.* **1991**, *15*, 153. (b) Philp, D.; Stoddart, J. F. *Angew. Chem., Int. Ed. Engl.* **1996**, *35*, 1154.
(18) Félix, O.; Hosseini, M. W.; De Cian, A.; Fischer, J. *Angew. Chem., Int. Ed. Engl.* **1997**, *36*, 102.
(19) Li, X.; Lah, M. S.; Pecoraro, V. L. *Inorg. Chem.* **1988**, *27*, 4657.

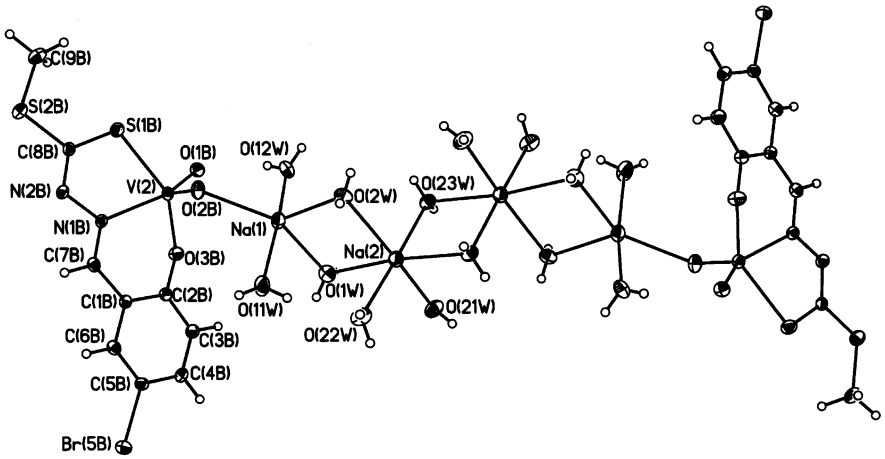

Figure 2. ORTEP drawing and crystallographic numbering scheme for the cationic part of complex $[(L^3VO_2Na)_2(H_2O)_7]_\infty$ (**1**).

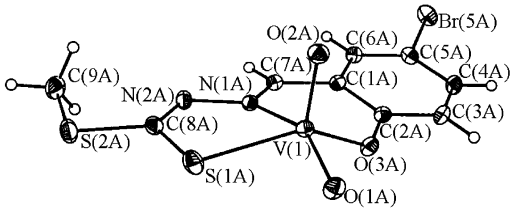

Figure 3. ORTEP drawing and crystallographic numbering scheme for the anionic part of complex $[(L^3VO_2Na)_2(H_2O)_7]_\infty$ (**1**).

is occupied by the remaining oxo atom O(3). The metrical parameters are similar to those in **1**. The L^1VO_2 unit is bound to the K^+ ion by both the terminal oxo atoms, the distances K−O(2) and K−O(3) being 2.874(2) and 2.974(2) Å, respectively.

An interesting aspect of this structure is the presence of seven-coordinated K^+ ion centers each acting as a bridge among three neighboring $L^1VO_2^-$ moieties (Figure 5). Besides O(2) and O(3) as described above, the remaining five coordination sites around K are occupied by the oxo groups O(2A) and O(3A), each belonging to a different but adjacent $L^1VO_2^-$ unit, phenoxo oxygen O(1A), and two bridging aqua ligands O(1W) and O(1WA) that help in the propagation of chain (Figure 4). All these K−O bonds have nearly identical lengths which fall in the range 2.714(2)−2.895(2) Å. In the process, the $L^1VO_2^-$ units here show a very interesting bonding behavior. While it binds a central K^+ ion in a chelated fashion (mode **II**) as mentioned above, it also bridges (mode **III**) two adjacent K^+ ions ($K^{\#1}$ and $K^{\#2}$) at the same time [O(2)−$K^{\#1}$, 2.895(2) and O(3)−$K^{\#2}$, 2.714(2) Å]. The distances K···$K^{\#1}$ and K···$K^{\#2}$ are identical 3.7921(8) Å. There are several secondary interactions in this molecule, viz. between O(1W)−O(2), O(1W)−O(3), and O(1W)−S(2), all through strong hydrogen bonds as listed in Table 3. These hydrogen-bonding interactions play a crucial role in stabilizing this extended structure with potassium ions forming an ion channel (Figure 5).

The molecular structure of $[L^2VO_2Rb(H_2O)]_\infty$ (**6**) also reveals an extended network. An ORTEP view of the monomeric unit is shown in Figure 6. Relevant metrical parameters are summarized in Table 4. One $L^2VO_2^-$ unit binds the Rb^+ ion through the terminal oxo groups O(2) and O(3) in a chelating fashion (mode **II**), the distances (Rb−O(2)/O(3)) being 2.9959(19) and 3.0111(19) Å, respectively. Three more coordination sites of Rb are occupied by an aqua ligand (Rb−O(1W), 2.943(2) Å), a sulfur atom from a second $L^2VO_2^-$ unit (3.4550(7) Å), and a nitro group oxygen O(5AD) (2.9601(19) Å) from a third $L^2VO_2^-$ group. In addition, Rb^+ is also attached to two distant nitro group oxygen atoms O(5AC) and O(5BC) both coming from a fourth oxovanadium unit (Figure 6), the distances being 3.169(2) and 3.261(2) Å, respectively. Thus, in all Rb has seven coordination sites in this molecule, contributed by four neighboring $L^2VO_2^-$ units and an aqua ligand. The Rb−O distances are within the range reported in the literature.[20−22] There are some hydrogen-bonding interactions in this molecule (Table 4) that help in stabilizing the extended network as shown in Figure 7.

A perspective view of the cesium complex $[L^1VO_2Cs]$ (**7**) is shown in Figure 8. The $L^1VO_2^-$ unit has distorted square pyramidal geometry (Figure 9) as observed in **1**, **3**, and **6**. The terminal V═O_t distances 1.624(9) and 1.628(8) Å and the included O(2)−V−O(3) angle 108.7(5)° (Table 5) are in the expected range.[19] Cs^+ ion is eight-coordinated here and connected to at least five $L^1VO_2^-$ units. One $L^1VO_2^-$ group utilizes its both terminal oxo atoms O(3B) and O(2B) as well as the phenoxo oxygen O(1B) to bind the alkali metal center, the Cs−O distances being 3.069(9), 3.133(9), and 3.197(8) Å, respectively (Figure 8). The later two oxygen atoms also act as bridge between the two neighboring Cs^+ ion centers, the distances being 3.762(9) and 3.545(9) Å, respectively. In addition, two more terminal oxo atoms, one each from two separate $L^1VO_2^-$ units, are also included in the Cs coordination sphere. One of these is an apical oxo atom O(3AB) while the other O(2AA) is an equatorial one, their distances from Cs being 3.013(9) and 3.054(4) Å, respectively. These, together with a sulfur atom S(1AA) from a fifth $L^1VO_2^-$ group complete the cesium coordination sphere (Cs−S, 3.627(3) Å). All the Cs−O distances are well within the range reported in the literature.[23] All these cross-

(20) Beattie, J. K.; Best, S. P.; Favero, P. D.; Skelton, B. W.; Sobolev, A. N.; White, A. H. *J. Chem. Soc., Dalton Trans.* **1996**, 1481.
(21) Devi, R. N.; Vidyasagar, K. *J. Chem. Soc., Dalton Trans.* **1998**, 3013.
(22) Bashall, A.; Beswick, M. A.; Harmer, C. N.; Hopkins, A. D.; McPartlin, M.; Paver, M. A.; Raithby, P. R.; Wright, D. S. *J. Chem. Soc., Dalton Trans.* **1998**, 1389.

Table 2. Selected Bond Distances (Å) and Angles (deg) for [(L^{3}VO$_2$Na)$_2$(H$_2$O)$_7$]$_\infty$ (**1**)[a]

Bond Lengths			
V(1)−O(2A)	1.620(3)	V(1)−O(1A)	1.652(3)
V(1)−O(3A)	1.914(3)	V(1)−N(1A)	2.167(3)
V(1)−S(1A)	2.3647(14)	V(2)−O(2B)	1.612(3)
V(2)−O(1B)	1.662(3)	V(2)−O(3B)	1.902(3)
V(2)−N(1B)	2.184(3)	V(2)−S(1B)	2.3691(14)
Na(1)−O(11W)	2.284(5)	Na(1)−O(2W)	2.352(4)
Na(1)−O(1W)	2.357(4)	Na(1)−O(12W)	2.387(5)
Na(1)−O(2B)	2.447(3)	Na(2)−O(23W)	2.383(4)
Na(2)−O(22W)	2.400(4)	Na(2)−O(21W)	2.405(5)
Na(2)−O(23W)$^{\#1}$	2.454(4)	Na(2)−O(1W)	2.461(5)
Na(2)−O(2W)	2.516(4)	Na(1)−Na(2)	3.566(3)
Na(2)−Na(2)$^{\#1}$	3.534(4)		

Bond Angles			
O(2A)−V(1)−O(1A)	107.8(2)	O(2A)−V(1)−O(3A)	109.3(2)
O(1A)−V(1)−O(3A)	94.61(14)	O(2A)−V(1)−N(1A)	100.21(14)
O(1A)−V(1)−N(1A)	150.9(2)	O(3A)−V(1)−N(1A)	83.01(12)
O(2A)−V(1)−S(1A)	107.37(12)	O(1A)−V(1)−S(1A)	87.28(12)
O(3A)−V(1)−S(1A)	140.64(10)	N(1A)−V(1)−S(1A)	77.00(9)
O(2B)−V(2)−O(1B)	107.7(2)	O(2B)−V(2)−O(3B)	105.1(2)
O(1B)−V(2)−O(3B)	96.28(14)	O(2B)−V(2)−N(1B)	100.24(14)
O(1B)−V(2)−N(1B)	151.0(2)	O(3B)−V(2)−N(1B)	83.43(13)
O(2B)−V(2)−S(1B)	107.85(13)	O(1B)−V(2)−S(1B)	87.29(11)
O(3B)−V(2)−S(1B)	144.01(11)	N(1B)−V(2)−S(1B)	76.86(10)
O(11W)−Na(1)−O(2W)	94.9(2)	O(11W)−Na(1)−O(1W)	79.7(2)
O(2W)−Na(1)−O(12W)	98.3(2)	O(1W)−Na(1)−O(12W)	92.2(2)
O(11W)−Na(1)−O(2B)	93.8(2)	O(2W)−Na(1)−O(2B)	125.6(2)
O(1W)−Na(1)−O(2B)	146.6(2)	O(2W)−Na(1)−O(1W)	87.8(2)
O(11W)−Na(1)−O(12W)	164.2(2)	O(12W)−Na(1)−O(2B)	85.4(2)
O(23W)−Na(2)−O(22W)	176.2(2)	O(23W)−Na(2)−O(21W)	83.5(2)
O(22W)−Na(2)−O(21W)	100.1(2)	O(22W)−Na(2)−O(23W)$^{\#1}$	97.7(2)
O(21W)−Na(2)−O(23W)$^{\#1}$	89.4(2)	O(23W)−Na(2)−O(1W)	97.7(2)
O(22W)−Na(2)−O(1W)	83.8(2)	O(21W)−Na(2)−O(1W)	86.0(2)
O(23W)$^{\#1}$−Na(2)−O(1W)	173.6(2)	O(23W)−Na(2)−O(2W)	87.1(2)
O(22W)−Na(2)−O(2W)	89.7(2)	O(21W)−Na(2)−O(2W)	163.6(2)
O(23W)$^{\#1}$−Na(2)−O(2W)	103.4(2)	O(1W)−Na(2)−O(2W)	82.01(14)

[a] Symmetry transformations used to generate equivalent atoms: (#1) $-x + 4, -y - 1, -z + 2$.

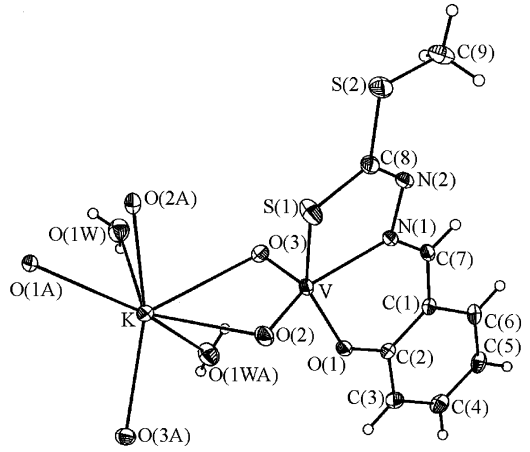

Figure 4. Molecular structure of the monomeric unit of [L^{1}VO$_2$K(H$_2$O)]$_\infty$ (**3**), showing the atom-labeling scheme.

connectivities and bridging coordination of the terminal oxo groups between the neighboring Cs^+ ions generate an infinite structural assembly forming cesium ion channels as shown in Figure 10.

Electronic Spectroscopy. Electronic spectra of the complexes **1**−**7** were recorded in CH_3CN. Relevant data are summarized in Table 6. All these complexes display an intense to medium-intensity (ϵ, 6800−14 600 mol^{-1} cm^2) band in the near-UV region (410−377 nm), the position of which is tunable by the substituent X (X = H, NO_2, and Br)

Table 3. Selected Bond Distances (Å) and Angles (deg) for [L^{1}VO$_2$K(H$_2$O)]$_\infty$ (**3**)[a]

Bond Lengths (Å)			
V−O(3)	1.622(2)	V−O(2)	1.651(2)
V−O(1)	1.924(2)	V−N(3)	2.180(2)
V−S(1)	2.3846(8)	K−O(3)$^{\#1}$	2.714(2)
K−O(1W)	2.800(3)	K−O(1)$^{\#2}$	2.824(2)
K−O(2)	2.874(2)	K−O(1W)$^{\#1}$	2.894(3)
K−O(2)$^{\#2}$	2.895(2)	K−O(3)	2.974(2)
O(3)−K$^{\#2}$	2.714(2)	O(2)−K$^{\#1}$	2.895(2)
O(1)−K$^{\#1}$	2.824(2)	O(1W)−K$^{\#2}$	2.894(3)
K−K$^{\#1}$	3.7921(8)	K−K$^{\#2}$	3.7921(8)

Bond Angles (deg)			
O(3)−V−O(2)	107.07(10)	O(1)−V−O(3)	106.95(9)
O(2)−V−O(1)	95.09(9)	O(3)−V−N(1)	102.97(9)
O(2)−V−N(1)	149.00(9)	O(1)−V−N(1)	83.22(7)
O(3)−V−S(1)	101.37(7)	O(2)−V−S(1)	89.68(7)
O(1)−V−S(1)	148.40(6)	N(1)−V−S(1)	76.95(5)
O(3)−V−K	55.23(8)	O(2)−V−K	51.84(7)
O(1)−V−K	108.38(5)	N(1)−V−K	157.12(6)
O(1W)−K−O(2)	128.59(7)	O(3)$^{\#1}$−K−O(1W)$^{\#1}$	77.92(8)

Hydrogen Bonding Parameters (Å, deg)

D−H···A	*d*(D−H)	*d*(H···A)	*d*(D···A)	∠DHA
O(1W)−H(2W) ···O(2)$^{\#3}$	0.82(6)	2.40(6)	3.156(3)	154(5)
O(1W)−H(1W) ···O(3)$^{\#2}$	0.72(7)	2.55(6)	3.047(4)	128(6)
O(1W)−H(1W)···S(2)$^{\#4}$	0.72(7)	2.99(6)	3.620(3)	147(6)

[a] Symmetry transformations used to generate equivalent atoms: (#1) $x + 1/2, y, -z + 1/2$; (#2) $x - 1/2, y, -z + 1/2$; (#3) $-x, y - 1/2, -z + 1/2$; (#4) $-x - 1, y - 1/2, -z + 1/2$.

(23) Cunningham, D.; McArdle, P.; Mitchell, M.; NiChonchubhair, N.; O'Gara, M.; Franceschi, F.; Floriani, C. *Inorg Chem.* **2000**, *39*, 1639.

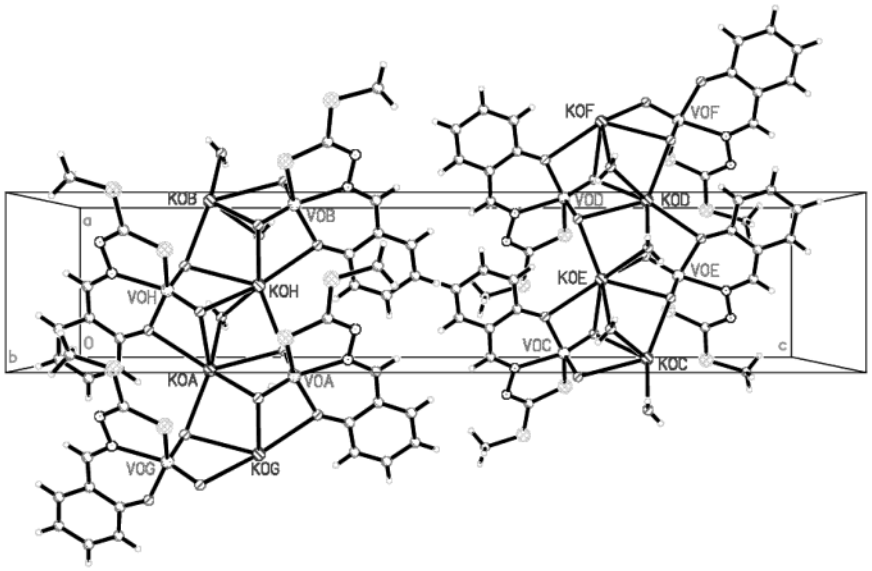

Figure 5. Hydrogen-bonded extended chain structure of **3**, viewed along the *a* axis.

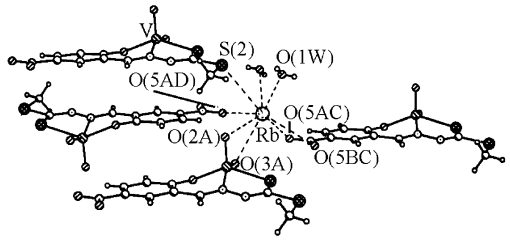

Figure 6. ORTEP plot and the atom numbering scheme for the monomeric unit of $[L^2VO_2Rb(H_2O)]_\infty$ (**6**).

Table 4. Selected Bond Distances (Å) and Angles (deg) for $[L^2VO_2Rb(H_2O)]_\infty$ (**6**)[a]

Bond Lengths			
Rb−O(1W)	2.943(2)	Rb−O(5AD)	2.9601(19)
Rb−O(5AC)	3.169(2)	Rb−O(5BC)	3.261(2)
Rb−O(2)$^{\#2}$	2.9959(19)	Rb−O(3)$^{\#2}$	3.0111(19)
Rb−O(1W)$^{\#3}$	3.050(2)	Rb−N(5)$^{\#1}$	3.412(2)
V−O(2)	1.6297(18)	V−O(3)	1.6563(18)
V−O(1)	1.9023(19)	V−N(1)	2.209(2)
V−S(1)	2.3714(7)	V− Rb$^{\#5}$	1.741(2)

Bond Angles			
O(2)−V−O(3)	107.12(9)	O(2)−V−O(1)	109.56(8)
O(3)−V−O(1)	97.89(9)	O(2)−V−N(1)	98.00(8)
O(3)−V−N(1)	153.28(8)	O(1)−V−N(1)	81.77(8)
O(2)−V−S(1)	105.00(7)	O(3)−V−S(1)	87.12(7)
O(1)−V−S(1)	141.69(6)	N(1)−V−S(1)	77.52(6)
O(1W)− Rb−O(5AD)$^{\#1}$	128.85(6)	O(1W)− Rb−O(5AD)$^{\#4}$	134.08(6)

Hydrogen Bonding Parameters (Å, deg)

D−H···A	*d*(D−H)	*d*(H···A)	*d*(D···A)	∠DHA
O(1W)− H(1W1)···O(3)$^{\#7}$	0.81(4)	2.00(4)	2.807(3)	174(4)
O(1W)− H(1W2)···S(1)$^{\#3}$	0.67(4)	2.91(4)	3.518(2)	154(4)

[a] Symmetry transformations used to generate equivalent atoms: (#1) *x*, *y* − 1, *z* + 1; (#2) *x*, *y* −1, *z*; (#3) −*x* + 1, −*y* + 2, −*z* + 2; (#4) −*x* + 2, −*y* + 3, −*z* + 1; (#5) *x*, *y* + 1, *z* − 1; (#6) *x*, *y* + 1, *z* − 1; (#7) *x* − 1, *y* − 1, *z*.

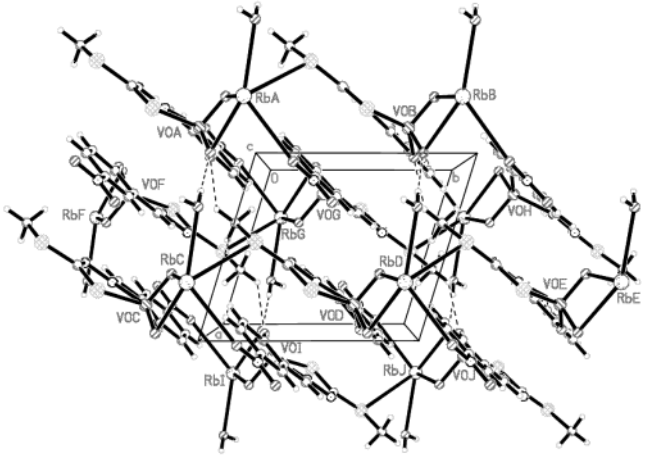

Figure 7. Packing diagram of **6** showing the extended structure.

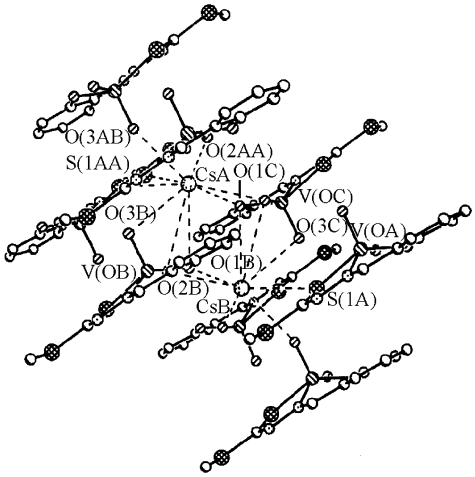

Figure 8. Perspective view of complex $[L^1VO_2Cs]_\infty$ (**7**) showing the cesium coordination environment.

in the phenyl ring of the tridentate ONS ligand. We interpret this band as arising from a ligand-to-metal charge-transfer (LMCT) transition from phenolate oxygen to an empty d orbital of vanadium(V). All the remaining bands appearing in the UV region are due to ligand internal transitions.

^{1}H NMR Spectroscopy. ^{1}H NMR spectra of the complexes were recorded in acetonitrile-d_3 and methanol-d_4. The spectrum of **3** in methanol-d_4 is shown in Figure 11 as a prototype. The spectral data in acetonitrile-d_3 are summarized in Table 7. The free ligands display a couple of broad resonances within a narrow range between 10.5 and 11.0

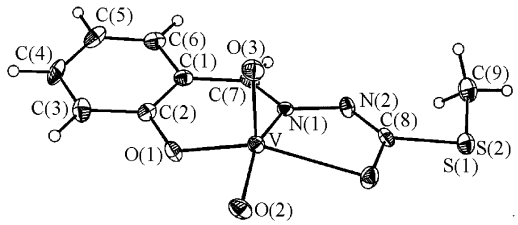

Figure 9. ORTEP plot and the atom numbering scheme for the $L^1VO_2^-$ unit in **7**.

Table 5. Selected Bond Distances (Å) and Angles (deg) for $[L^1VO_2Cs]_\infty$ (**7**)[a]

	Bond Lengths		
V−O(3)	1.624(9)	V−O(2)	1.628(8)
V−O(1)	1.922(9)	V−N(1)	2.188(9)
V−S(1)	2.350(4)	Cs−O(2)$^{\#1}$	3.054(9)
Cs−O(3)$^{\#2}$	3.063(9)	Cs−O(3)	3.103(9)
Cs−O(2)$^{\#3}$	3.133(9)	Cs−O(1)$^{\#1}$	3.197(8)
Cs−O(1)	3.545(9)	Cs−S(1)$^{\#3}$	3.627(3)
Cs−S(1)$^{\#4}$	3.680(4)	Cs−O(2)	3.762(9)
Cs−S(2)$^{\#4}$	4.030(4)	O(1)− Cs$^{\#1}$	3.197(8)
	Bond Angles		
O(3)−V−O(2)	108.7(5)	O(3)−V−O(1)	104.9(4)
O(2)−V−O(1)	94.4(4)	O(3)−V−N(1)	99.3(4)
O(2)−V−N(1)	151.8(4)	O(1)−V−N(1)	82.0(4)
O(3)−V−S(1)	107.7(4)	O(2)−V−S(1)	90.1(4)
O(1)−V−S(1)	143.6(3)	N(1)−V−S(1)	77.3(3)
O(2)$^{\#1}$−Cs−O(3)$^{\#2}$	145.8(3)	O(2)$^{\#1}$−Cs−O(3)	126.2(2)
O(3)−Cs−O(1)	49.6(2)	O(3)−Cs−O(2)	44.0(2)
O(1)−Cs−O(2)	41.77(18)	O(1)−Cs−V	30.05(14)

[a] Symmetry transformations used to generate equivalent atoms: (#1) $-x-1, -y+1, -z$; (#2) $-x, -y+1, -z$; (#3) $x, y, z-1$; (#4) $-x, -y+1, -z+1$; (#5) $x, y, z+1$.

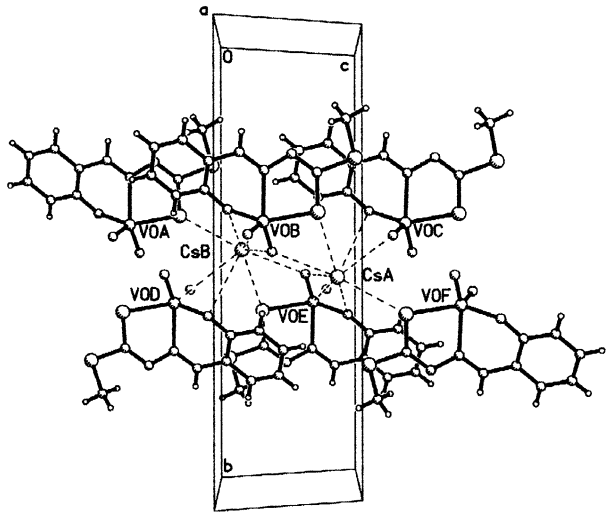

Figure 10. Molecular structure for the complex $[L^1VO_2Cs]_\infty$ (**7**) viewed along the *c* axis, demonstrating the infinite chain forming ion channel.

ppm, due to phenolic OH and NH protons which are missing in the complexes. Also the azomethine (H_5) and phenyl ring (H_1) protons in the complexes are shifted downfield relative to those in the free ligands.[2] This indicates participation of phenolate oxygen and imino nitrogen in vanadium-ligand attachment as established in the solid state by X-ray crystallography.

In dry CH_3CN, DMF, or DMSO, the solutions of **1**−**7** are photoreactive. Fresh yellow solutions are gradually changed to green with the exposure to visible light. The progress of such photochemical reaction has been monitored by ^1H NMR spectroscopy, and the results obtained with a representative compound **1** are shown in Figure 12. Gradual loss of resolution as well as line-broadening of the spectral features are observed in all the cases with the elapse of exposure time. This indicates generation of paramagnetic species through photochemical process as established by several control experiments.[2]

Table 6. Electronic Spectral Data for the Complexes (**1**−**7**) in CH_3CN Solution

complex	λ_{max}, nm (ϵ, $mol^{-1}\,cm^2$)
1	410 (8038); 285 (20 200); 235 (27 100)
2	377 (14 600); 312 (22 500); 231 (22 900)
3	378 (11 800); 310 (18 000); 230 (18 200)
4	401 (8700); 285 (21 800); 235 (29 300)
5	393 (9000); 285 (22 600); 234 (28 400)
6	379 (13 900); 311 (21 400); 231 (21 600)
7	394 (6800); 286 (16 700); 232 (20 900)

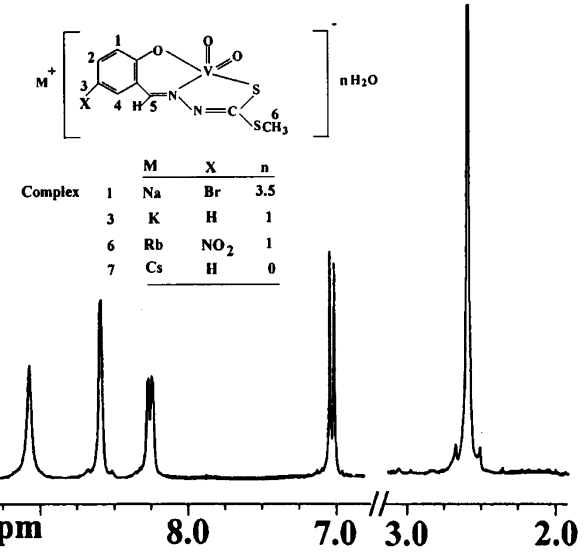

Figure 11. 300 MHz ^1H NMR spectrum of **3** in methanol-d_4 solution at 25 °C.

Identification of Photolysis Products. Despite our best efforts, isolation of the photoreduced products **1a**−**7a** (corresponding precursor complexes being **1**−**7**) in the solid state remained elusive. The green paramagnetic products, unlike their precursors, are EPR active. A representative spectrum (**3a**), obtained by the photoreduction of **3**, is displayed in Figure 13 involving a 15-line feature at room temperature with $\langle g \rangle = 1.99$ (1.96 for **1a**). The results indicate the presence of a coupled vanadium ($I = 7/2$) center with an odd interacting electron. The hyperfine splitting parameter $\langle A \rangle_{15}$, 44.5×10^{-4} cm^{-1} (46.4×10^{-4} cm^{-1} for **1a**), is almost half as much as that of a localized spectrum ($\langle A \rangle_8$, 89×10^{-4} cm^{-1}) reported elsewhere for a (μ-oxo)-divanadium(IV/V) compound with similar ligand.[3] This again speaks in favor of **1a**−**7a** to be dinuclear vanadium(IV/V) compounds[24] with mutually interacting metal centers as reported earlier.[3,4]

In compliance with their proposed mixed-oxidation status, the photoreduced species **1a**−**7a** display an intervalence

(24) Slichter, C. P. *Phys. Rev.* **1955**, *99*, 478.

Table 7. ^{1}H NMR Spectral Data (δ, ppm)[a] for the Vanadium(V) Complexes (**1**−**7**) in Acetonitrile-d_3 at 25 °C

1		3		6		7		assgnt
8.94 s	1 H	8.98 s	1 H	9.08 s	1 H	8.94 s	1 H	H_5
7.68 s	1 H	7.59 d (8.30)	1 H	8.60 s	1 H	7.55 d (6.93)	1 H	H_4
		7.47 t (7.90)	1 H			7.45 t (7.90)	1 H	H_3
7.50 d (8.82)	1 H	6.98 d (8.98)	1 H	8.28 d (7.08)	1 H	6.92 d (7.69)	1 H	H_1
6.86 d (8.89)	1 H	6.92 s	1 H	7.05 d (9.24)	1 H	6.87 s	1 H	H_2
2.57 s	3 H	2.58 s	3 H	2.60 s	3 H	2.56 s	3 H	H_6

[a] Chemical shifts against internal TMS. Proton labels are shown in Figure 11. Key: s, singlet; d, doublet; t, triplet. Values in the parentheses represent coupling constants (J in Hz).

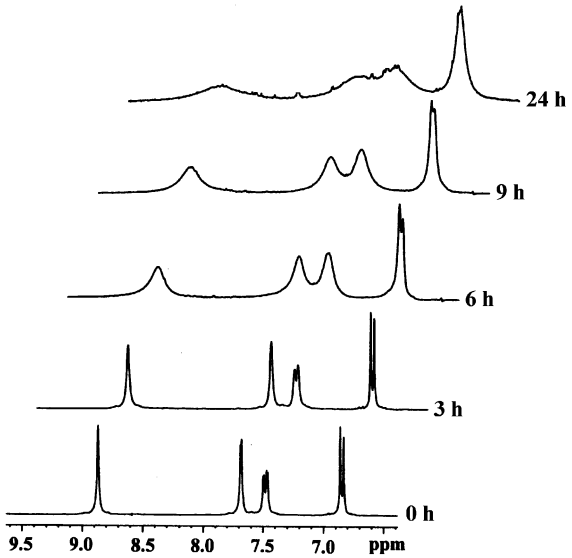

Figure 12. Time-dependent ^{1}H NMR spectra of **1** in acetonitrile-d_3 solution under the exposure of visible light, showing gradual line-broadening.

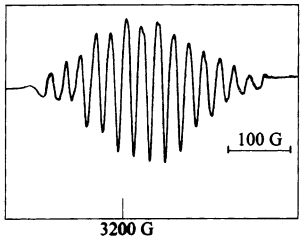

Figure 13. X-band EPR spectrum at room temperature of the photoreduced product **3a** in CH_3CN/toluene (1:1.5, v/v) after 12 h exposure to visible light.

charge-transfer (IT) band in the near-IR region (955−970 nm) of their electronic spectra in solution. A representative spectrum (**3a**) is shown in Figure 14. It involves an IT band at 967 nm, followed by a low-intensity shoulder, centered around 664 nm, the intensity ratio A_{967}/A_{664} being close to 1.5 after 12 h exposure time. We believe this shoulder is due to a combination of overlapping ligand field bands, expected to arise for the oxovanadium(IV) center[25] of the putative mixed-oxidation divanadium(IV/V) product.

Unlike their precursors, the photoreduced products (**1a**−**7a**) are electrochemically active in the potential range −1.0 to +1.0 V vs SCE. They display an oxidation process, the current heights of which increase with the increase in exposure time as shown in Figure 15 for a representative precursor compound **3**. This indicates gradual accumulation

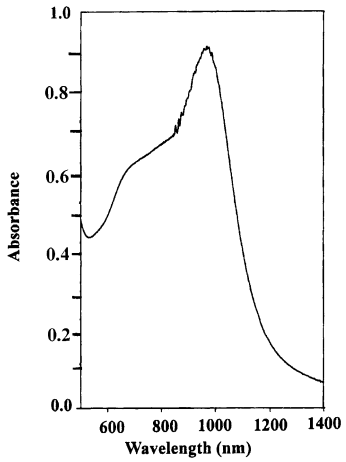

Figure 14. Electronic absorption spectrum of the photoreduced product **3a** in acetonitrile solution, recorded after 12 h of exposure to visible light.

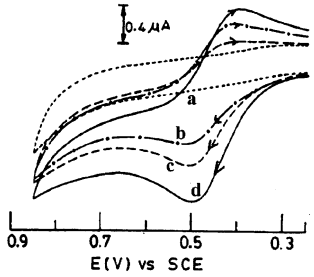

Figure 15. Cyclic voltammograms recorded with a solution of **3** in dry acetonitrile during the progress of photoreduction: (a) fresh solution; (b) after 1 h, (c) after 3 h, and (d) after 12 h of exposure to visible light.

of the electroactive species in solution with the increase in exposure time to visible radiation. On the basis of comparison with ferrocenium/ferrocene couple (ΔE_p, 80 mV, and i_{pa}/i_{pc}, 1.0, at 50 mV s^{-1}), this oxidation process (ΔE_p, 85 mV, and i_{pa}/i_{pc}, 1.1, at 50 mV s^{-1}) may be described as reversible[26] involving single-electron transfer. The $E_{1/2}$ value for this process with **3a** is 0.44 V which suffers a 60 mV positive shift in the case of **1a** ($E_{1/2}$, 0.50 V). The electrochemical results thus indicate the presence of an oxidizable vanadium-(IV) center in the photoreduced product $[LOV^{IV-}O-V^{V}OL]^-$ that undergoes one-electron transfer (eq 1) with $E_{1/2}$ value tunable by the substituent X present in the aromatic ring of the ligand framework (L).

$$[LOV^{V-}O-V^{IV}OL]^- \overset{-e^-}{\rightleftharpoons} [LOV^{V-}O-V^{V}OL]^0 \quad (1)$$

(25) Selbin, J. *Chem. Rev.* **1965**, *65*, 153.

(26) Brown, E. R.; Large, R. F. In *Electrochemical Methods*; Weissberger, A., Rossiter, B., Eds.; Physical Methods in Chemistry; Wiley-Interscience: New York, 1971; Part IIA, ChapterVI.

Chart 2

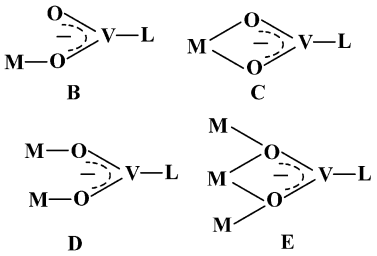

The results of EPR, electronic spectral, and electrochemical studies thus indicate the generation of a (μ-oxo)divanadium(IV/V) species [LVO−(μ-O)−OVL]$^-$ as the putative product of photoreduction in dry acetonitrile solution.

Concluding Remark. The coordinating abilities of LVO_2^- species as an "inorganic analogue" of carboxylate functionality[2,27] have been explored. All the alkali metal ions, except lithium, form adducts that show interesting variations in their solid-state structures as confirmed by X-ray crystallography. Like carboxylate, the LVO_2^- moieties here have adopted various binding patterns (Chart 2) with the change of alkali metal ions. With sodium ion in **1**, the mode of attachment is monodentate (**B**), while, with rubidium in **6**, a chelating mode (**C**) is observed. With potassium and cesium however, the mode of attachment is much more complicated (**E** type) as observed in **3** and **7**, respectively. These attachment modes are not only controlled by the size of the alkali metal ions but also by the steric bulk of the associated tridentate ligand (L). Recently we reported a sodium compound $[L^1VO_2Na(H_2O)_2]_\infty$ with H_2L^1 as the tridentate ligand that displayed an interesting single-stranded helical structure with $L^1VO_2^-$ unit showing the bis-monodentate type (**D**) of attachment. Strong electrostatic and hydrogen bonding interactions play the central role in stabilizing these extended structures in the solid state.

In solution of aprotic solvents of high donor strengths, viz. CH_3CN, DMF, or DMSO, these hydrogen-bonded extended structures dissociate, possibly due to solvent interventions[28−30] that render the LVO_2^- units susceptible to undergo proton-coupled photoinduced one-electron reduction through the intermediate formation of a hydroxo $LV^VO(OH)$ species[31,32] (eqs 2 and 3). The $LV^{IV}O$ species thus generated reacts with excess $LV^VO_2^-$ species, leading to the formation of a μ-oxo mixed-oxidation divanadium(IV/V) product (eq 4).[33] One unit of negative charge carried by the LVO_2^- species here, we believe, is very important as it favors the protonation process, the first step of this photochemical transformation. Structurally characterized mixed-oxidation poly(oxo)vanadates(IV/V), prepared by photochemical reduction, have been reported recently in the literature.[34]

$$LV^VO_2^- + H^+ \rightleftharpoons LV^VO(OH) \quad (2)$$

$$LV^VO(OH) + H^+ + e^- \overset{h\nu}{\rightleftharpoons} LV^{IV}O + H_2O \quad (3)$$

$$LV^{IV}O + LV^VO_2^- \rightleftharpoons [LV^{IV}O{-}(\mu\text{-}O){-}OV^VL]^- \quad (4)$$

Acknowledgment. Financial support received from the Council of Scientific and Industrial Research (CSIR), New Delhi, is gratefully acknowledged. D.M. also thanks the CSIR for the award of a Junior Research Fellowship.

Supporting Information Available: X-ray crystallographic files in CIF format for compounds **1**, **3**, **6**, and **7**. This material is available free of charge via the Internet at http://pubs.acs.org.

IC030080I

(27) Pasquali, M.; Marchetti, F.; Floriani, C.; Cesari, M. *Inorg. Chem.* **1980**, *19*, 1198.
(28) Rebek, J., Jr. *Angew. Chem., Int. Ed. Engl.* **1990**, *29*, 245.
(29) Whitesides, G. M.; Mathias, J. P.; Seto, C. T. *Science* **1991**, *254*, 1312.
(30) Fan, E.; Van Arman, S. A.; Kincaid, S.; Hamilton, A. J. *J. Am. Chem. Soc.* **1993**, *115*, 369.
(31) Root, C. A.; Hoeschele, J. D.; Cornman, C. R.; Kampf, J. W.; Pecoraro, V. L. *Inorg. Chem.* **1993**, *32*, 3855.
(32) Asgedom, G.; Sreedhara, A.; Kivikoski, J.; Kolehmainen, E.; Rao, C. P. *J. Chem. Soc., Dalton Trans.* **1996**, 93.
(33) Nishizawa, M.; Hirotsu, K.; Ooi, S.; Saito, K. *J. Chem. Soc., Chem. Commun.* **1979**, 707.
(34) Yamase, T.; Suzuki, M.; Ohtaka, K. *J. Chem. Soc., Dalton Trans.* **1997**, 2463.